Materials and Structures
DOI 10.1617/s11527-012-9994-z

ORIGINAL ARTICLE

Temperature and humidity influences on the on-site active marine corrosion of reinforced concrete elements

Y. A. Villagrán Zaccardi · A. Bértora · A. A. Di Maio

Received: 24 February 2012 / Accepted: 29 November 2012

Abstract Reinforcement corrosion is a main durability issue for reinforced concrete structures in the marine environment. Environmental actions on the corrosion rate have been documented by several researchers on actively corroding reinforced concrete structures. Therefore, considering the influences of ambient temperature and relative humidity is very important for prospective studies of corroding structures. In this paper, active corrosion of concrete members in the marine environment was observed for 4.8 years, and a relationship between the corrosion rate and ambient temperature and relative humidity is modeled. This very simple proposal is presented as a complementary tool to experimental measurements when assessing the deterioration rate of concrete structures in the marine environment.

Keywords Reinforced concrete · Corrosion · Chloride · Temperature · Humidity

Abbreviations

Δ_{st}	Variation due to seasonal effects (mV)
b	Coefficient for sine function (mV)
B	The Tafel slope (mV)
BPC	Blended portland cement
c	Increasing coefficient for i_{corr} [$\mu A/(cm^2 \cdot month)$]
CSE	$Cu/CuSO_4$ electrode
$E_{corr,est}$	Estimated half-cell potential (mV)
$E_{corr,mean}$	Average half-cell potential of the whole exposure period (mV)
I_{corr}	Corrosion current (μA)
i_{corr}	Corrosion rate ($\mu A/cm^2$)
$i_{corr,0}$	Balanced initial corrosion rate ($\mu A/cm^2$)
r	Scaling coefficient for b [$\mu A/(cm^2 \cdot mV)$]
RH	Relative humidity
R_p	Polarization resistance ($k\Omega$)
t	Exposure time (months)
t_o	Time displacement (months)
TRH	Temperature multiplied by RH [°C· %]

Y. A. Villagrán Zaccardi (✉) · A. Bértora · A. A. Di Maio
LEMIT, 52 entre 121 y 122 s/n, 1900 La Plata, Argentina
e-mail: yuryvillagran@conicet.gov.ar

Y. A. Villagrán Zaccardi · A. Bértora · A. A. Di Maio
CONICET, Buenos Aires, Argentina

Published online: 13 December 2012

1 Introduction

The marine environment is highly aggressive to reinforced concrete. A main aggressive action is caused by the presence of salt in the atmosphere, which leads to corrosion of steel in concrete. Though steel forms a passive layer when embedded in sound concrete, a critical chloride content causes pitting in the passive layer, and steels starts corroding actively. This is known as the chloride threshold content.

The marine atmosphere is one of the zones of exposure that can be defined in the marine environment, where concrete is never in direct contact with seawater but with a marine aerosol [1]. Other marine zones are the splash and the submerged zones. Each zone differs from the others on the mechanisms of chloride ingress into concrete and the saturation degree of concrete. Concrete in any of these zones is affected by ambient temperature, but ambient relative humidity (RH) has greater impact on concrete when in the marine atmosphere than when in the other exposure zones.

The corrosion process develops through anodic and cathodic zones, leading to corrosion cells with a certain open circuit cell voltage. The half-cell potential corresponding to the working electrode, i.e. the reinforcing steel, is assessed by voltage measurements against a reference electrode (e.g., versus Cu/$CuSO_4$ electrode, CSE).

In the field, the interpretation of the value of the half-cell potential may be done according to ASTM C876 (ASTM C876 2009) [2]. These limits were devised empirically from salt induced corrosion of cast-in-place bridge decks in the USA [3]. Other criteria have also been established to define a corrosion risk on the basis of the half-cell potential (Table 1). Half-cell potential measurements are indicative of the corrosion risk of steel in concrete, but prospecting is not simple.

Besides, the kinetics of corrosion may be assessed by electrochemical measurements of the polarization resistance (R_p). The value of R_p is inversely proportional to the corrosion current (I_{corr}) (Eq. 1), and its equivalent per unit area, corrosion rate (i_{corr}). Where B is the Tafel slope (equal to 26 or 52 mV in the passive or active states, respectively). The polarization resistance can be measured by implementing potential signals on reinforced concrete and registering the current response (potentiostatic method) [5]

$$I_{corr} = \frac{B}{R_p} \quad (1)$$

The corrosion rate refers to the rate of volumetric growth of corrosion products, and it is therefore indicative of the propagation period. Its practical use includes the estimation of the period after which particular pathologic manifestations in the structure can be expected (Table 2). However, its value is not constant, and prospective techniques must account for the influence of the environment.

Saturated concrete is characterized by low resistivity and slow oxygen diffusion. Therefore, the cathodic process controls the corrosion rate. With increasing saturation degree, the corrosion rate is limited by oxygen availability and rust reduction. In unsaturated conditions, the corrosion rate of active embedded steel is governed by concrete resistivity, in direct connection with its moisture content [6]. Therefore, the saturation degree of cover concrete is a key factor when studying reinforcement corrosion.

In this sense, the moisture content of concrete is one of the most influencing parameters in the value of the half-cell potential in reinforced concrete structures [7, 4]. Lack of oxygen in the saturated state can lead to very negative values of the half-cell potential [3]. Whereas the potential may be near +100 mV versus CSE in aerated concrete, values of −400 and −900 mV versus CSE are possible when concrete is

Table 1 Corrosion risk according to E_{corr}

Vs. CSE	Corrosion risk	
E_{corr} (mV)	Stratfull (bridge decks) [4] (%)	ASTM (ASTM C876 2009) [2] (%)
−200	0	10
−240		
−275	5	
−350	50	90
−450	95	
−500	100	

Table 2 Expectable periods for damage

i_{corr} (μA/cm^2)	Ref. [8] Corrosion rate	Ref. [9] Structure evaluation
	Negligible	No expectable damage
0.1		
	Low	
0.2		
		Expectable damage in 10–15 years
0.5		
	Moderate	
1.0		
	High	Expectable damage in 2–10 years
10.0		
		Expectable damage before 2 years

saturated or there is a total absence of oxygen, respectively [6].

Concrete in the marine atmosphere is subjected to climatic variations in temperature and RH. These two parameters affect the corrosion rate of active reinforcement, especially by affecting the moisture content in concrete. López and González [10] linked the degree of pore saturation of concrete with the corrosion kinetics of steel in the active state. They obtained quantitative relations between the corrosion rate of reinforcement and the degree of pore saturation and resistivity of mortars. A critical practical pore saturation value was identified, below which the corrosion rate was too small to pose any durability problem.

Enevoldsen et al. [11] performed simultaneous measurements of corrosion rate, electrical resistivity and internal RH on concrete specimens. The corrosion rate was found to be strongly dependent on the electrical resistivity of the mortar or cover concrete. The electrical resistivity is, in turn, determined by the RH and the concentration of chlorides in the pore solution. They also suggest the existence of a threshold limit of the RH below which a significant corrosion current cannot be supported. The relationship between ambient RH and internal RH of concrete is shown as an important analysis tool.

Andrade et al. [12] studied the influences of humidity and temperature on the corrosion rate of reinforcement in mortar. They found a multiple simultaneous effect of the variation of temperature on different parameters (oxygen content, pH, chloride content) which may counter-balance each other. They recommend resistivity to be the best descriptor of the relationship between the corrosion rate and humidity in concrete.

It is therefore very important to state a methodology to assess the influence of climate when analyzing the value of the half-cell potential and the corrosion rate in a reinforced concrete structure.

The methodology proposed in the present paper for the analysis of electrochemical corrosion parameters is based on the quantification of the influences of the ambient temperature and RH on the deterioration rate. Climatic actions may be considered in two orders: daily variations and seasonal variations. In regard to their effect on reinforcement corrosion, the last are more important to be concerned with due to the period of the cycle involved. Daily variations cycles are not expected to show major practical effects, and only mean daily values are considered in this first approach.

This improved prospection tool for actively corroding structures includes a variable deterioration rate in connection with climate exposure conditions, and it supposes increased accuracy in comparison with a constant deterioration rate. Moreover, the use of this methodology may allow reducing the number of in situ measurements that are required to pursue the deterioration rate of a concrete structure in the marine environment.

2 Experimental

Five reinforced concrete members of 150 × 150 × 500 mm were studied. They were reinforced with four bars of 12 mm diameter in each edge and stirrups of 4.2 mm diameter spaced at 140 mm. Cover concrete was of low depth (<5 mm) in order to reach fast depassivation. Thus, all presented data correspond to the propagation period of corrosion.

Cylindrical compressive strength at 28 days of concrete was 26 MPa, with a water-to-cementitius-material ratio of 0.60 and a unitary cement content of 280 kg/m^3. A blended Portland cement (BPC) admixed with limestone filler [17 % of cement weight (c.w.)] and slag (12 % of c.w.), was used. The properties of BPC are listed in Table 3.

Reinforced steel was used with minimal rust, but no special surface treatment was applied prior to concreting. This was intended to obtain representative data of real reinforced concrete structures, in which

Table 3 Chemical and physical properties of BPC

Properties	BPC
Blaine specific surface (m^2/kg)	338
Density	3.03
Chemical analysis (%)	
Loss on ignition	3.00
Insoluble residue	2.70
SO_3	1.87
MgO	0.95
SiO_2	19.00
Fe_2O_3	3.88
Al_2O_3	7.37
CaO	60.95
Chloride	0.011

the surface of steel is usually not completely free of rusting.

Reinforced concrete members were cast in the direction of their main axis. Therefore, capillary pores orientation was parallel to the longest dimension, and it should not be expected differences due to the casting direction between results from each of the four long sides of the specimens. Concrete elements were cured in a fog room for 28 days and then exposed to a marine environment.

The exposure site was at about 50 m from the coastline in a rural area near Mar del Plata city, Argentina (Figs. 1, 2). Long axis of the specimens was set perpendicularly to the coastline. Thus, a top side (A), two lateral sides (B and D), and a bottom side (C) were set up for each concrete member.

Fig. 1 Exposed reinforced concrete members

Fig. 2 Exposure zone

Half-cell potentials and corrosion rates were regularly measured during 4.8 years of exposure. Corrosion rate was assessed by the use of a corrosimetre device with a guard ring, which operates the polarization resistance method previously described. Three measurements (in the middle and at both ends) were performed on each of the four long faces of the elements. This amounts to 60 individual values for each measurement time.

3 Results

Mean values and standard deviations for half-cell potential and corrosion rate measurements performed for exposure periods of 0, 12.4, 17.5, 26, 33.4, 42.1 and 57.8 months are shown in Fig. 3. Exposure started on 14 June. Therefore, $t = 0.23$ months agrees with the beginning of the winter season (21 June).

In Fig. 4, it can be seen that the dispersion of values decreases with the value of the mean half-cell potential. The oxygen availability at the steel surface, and thus the moisture content of concrete, primarily defines the electrochemical potential of the steel. If concrete is saturated, oxygen diffusivity through pore liquid will be decisive on the deterioration rate. Otherwise, the protection that the cover as resistive material may offer to steel acquires relevance. Being this the case, heterogeneities in the concrete member are highlighted by a wider range of values for the half-cell potential when concrete is dry.

Figure 5 shows the exposure periods of 17.5 and 42.1 months as those in which the most positive values

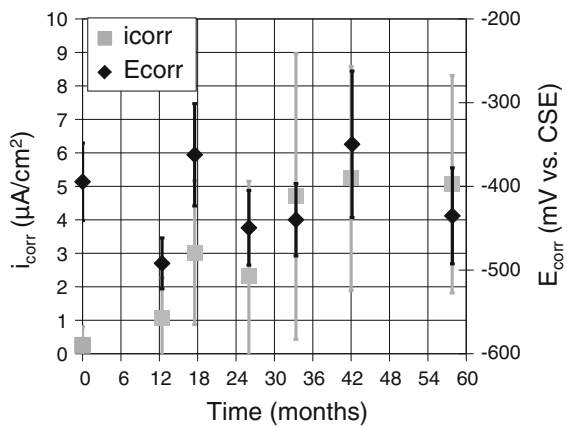

Fig. 3 Time evolutions of half-cell potential and corrosion rate

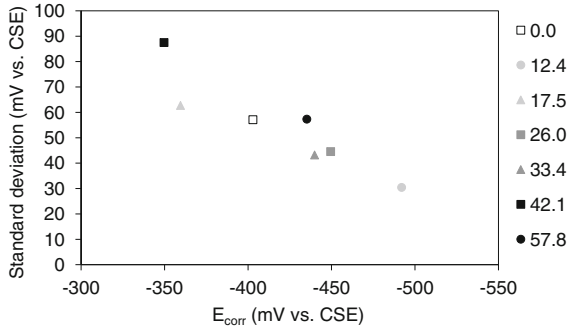

Fig. 4 Standard deviation of half-cell potentials

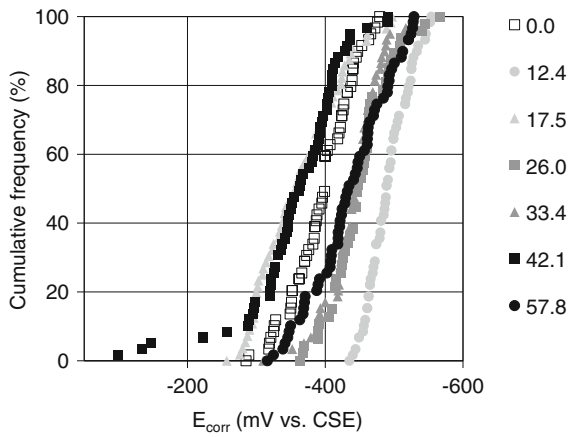

Fig. 5 Cumulative frequencies for the half-cell potential at different exposure periods

for the half-cell potential were obtained. In this two periods, 50 % of the measurements were more positive than −350 mV versus CSE, limit below which high corrosion risk is indicated in ASTM C876 (ASTM C876 2009) [2]. The values in the rest of exposure periods are mostly or completely below this limit. Accordingly, it is clear that steel remained active during the whole exposure period despite some values indicating intermediate risk levels. In the case of the corrosion rate, Fig. 6 shows that about 60 % of values for $t = 0$ are below 0.2 μA/cm^2. The rest of the initial measurements showed active values. This is related with the condition in which reinforcing steel was used. If any surface treatment would have been applied, fast passivation of steel would be expected. However, under the experimental conditions, the time required for steel to passivate seemed to be longer, corresponding to some instance between $0 < t < 12.4$ months. Unfortunately, this instance could not be completely

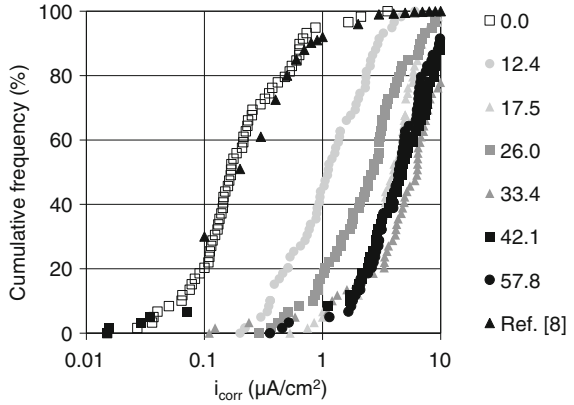

Fig. 6 Cumulative frequencies for the corrosion rate at different exposure periods

registered (it was detected only for 60 % of measurements) because depassivation occurred very early, before $t = 12.4$ months.

From Fig. 3 it can be seen that the average corrosion rate increases consistently with time. The highest values were at the latter exposure periods, with the highest individual measurements near 10 μA/cm^2, limit that is attributed to corrosion in the marine atmosphere [8].

The dispersion for the corrosion rate (Fig. 6) differs from that for the half-cell potential (Fig. 5). As well, in Fig. 3 it is noted that half-cell potential showed consistently annual cyclic values. The corrosion rate, in contrast, increased in value and dispersion along time.

4 Discussion

Ambient temperature and RH have simultaneous effects on the moisture content in concrete. Thus, it is convenient to consider their influence simultaneously and, therefore, the use of temperature multiplied by the RH (*TRH*), expressed in °C and %, respectively, seems practical. There are many other parameters that may be included in a very complex and detailed description, but then discrete weather events need to be considered, and they are hard to be included (and predicted) in a continuous formula.

If the half-cell potential is compared to *TRH*, a strong linear relationship is derived (Fig. 7). Thus, the value of the half-cell potential may be approximated with a linear relationship with *TRH*, and this simple parameter seems capable of empirically describe the

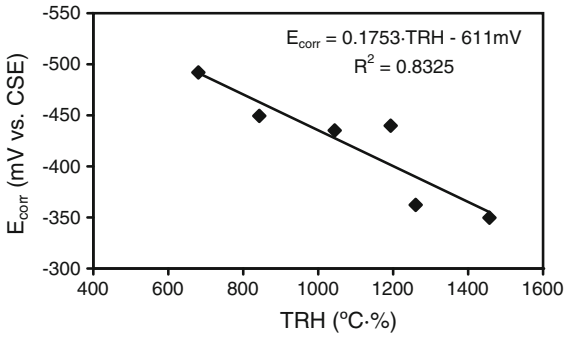

Fig. 7 Half-cell potential versus TRH

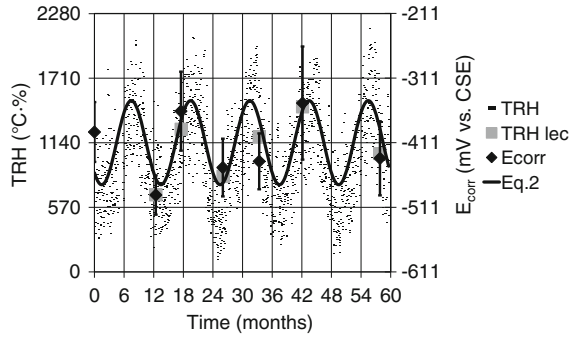

Fig. 8 Time evolution of the TRH parameter and the half-cell potential, and fit based on Eq. 2

influence of climatic exposure conditions. In addition, the annual variation of *TRH* is periodic, and can be modeled with a sine function. The proportionality between E_{corr} and *TRH* means that their evolutions in time replicate with a scaling difference.

Equation 2 offers a sine approach to the half-cell potential considering these two aspects. Where $E_{corr,est}$ is the estimated half-cell potential, $E_{corr,mean}$ is the average half-cell potential of the whole exposure period (equal to −411 mV for the collected data) and Δ_{st} is the variation due to seasonal effects calculated by Eq. 3. Where b is a coefficient reflecting the amplitude of the sine function (equal to 65 mV for the collected data), t_o is a value referring the time displacement of the sine function, and t is the exposure time (in months). The complete cycle is 12 months, starting on 5 November (middle of springtime), and with the maximum and minimum values for *TRH* at 3 and 9 months after this date. If the exposure starts on this date, $t_o = 0$. Considering the date for the starting of exposure, $t_o = 7.28$ months (from 5 November to 14 June). The highest value of *TRH* may not necessarily imply the lowest value for $E_{corr,est}$, due to a spare time that may be required for moisture to diffuse into concrete up to the reinforcement depth. This time is a function of the cover depth and its pore structure. For the presented data, this spare time was not taken into account considering that the low cover depth and high *w/c* of concrete allowed an early hygroscopic equilibrium between cover concrete and the environment. The presented data was collected while cover concrete remained sound, and Eq. 2 may need further modifications to be applied to cracked or delaminated reinforced concrete elements.

$$E_{corr,est} = E_{corr,mean} + \Delta_{st} \tag{2}$$

$$\Delta_{st} = b \cdot \sin\left(\frac{2\pi}{12\,\text{months}} \cdot (t_o + t)\right) \tag{3}$$

Figure 8 shows the evolution of the half-cell potential with time considered as a sine function of time with an annual period. Here, TRH_{lec} refers to the *TRH* value on the day of the experimental measurement of E_{corr}. Similarly to *TRH*, the more negative values for E_{corr} are those during the winter season, whereas the less negative occur in summer. Humidity in concrete pores is permanently towards equilibrium with the RH in the atmosphere, which determines the saturation degree of concrete. Concrete is drier during summer than winter, mainly due to high levels of sunshine and temperature. The seasonal variation of the half-cell potential is directly related to the moisture content of concrete. In Fig. 8, the initial measurement for E_{corr} does not fit into the sine evolution due to laboratory conditions, and a certain time of exposure

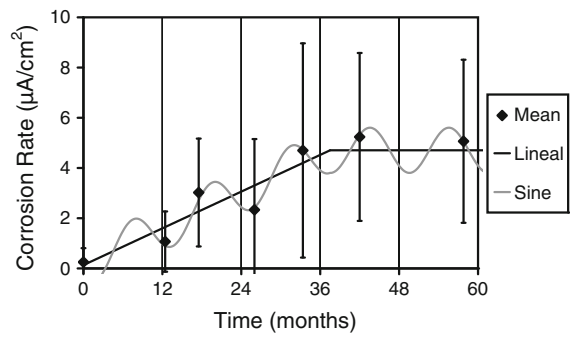

Fig. 9 Time evolution of the corrosion rate and fit based on Eq. 4

Fig. 10 Cracking patterns and rusting on reinforced concrete members

was necessary to have some environmental influence, mainly as regards moisture content.

The relationship presented to predict future values for the half-cell potential on the basis of ambient temperature and humidity seems very exciting. However, it is the corrosion rate evolution what matters in order to verify the loss of working section of reinforcement and the deterioration rate. For this

reason, this sine evolution is transposed to the variation of the corrosion rate.

However, the case of i_{corr} requires including an additional increasing term due to the progressive depassivation of a larger proportion of the steel surface with the increasing chloride content near the reinforcement. Therefore, the evolution of i_{corr} with time is analyzed by the time function in Eq. 4, consisting in the addition of three terms: an initial corrosion rate, an increasing term and a sine term (Fig. 9). Where $i_{corr,0}$ is the balanced initial corrosion rate, c an increasing coefficient (0.1219 μA/(cm^2·month) for the collected data), and r a scaling coefficient for b (72 μA/(cm^2·mV)). The sine term attains the highest (most positive) value in summer and the lowest (most negative) value in winter. This contrasts with E_{corr} in the sense that higher values for i_{corr} may be expected for more negative values of E_{corr}. Concrete reaches a higher saturation degree in winter, which decreases the availability of oxygen. As well, corrosion rate diminishes with lowering temperatures. Therefore, concrete is drier in summer than in winter, and the lower moisture content of concrete implies less negative values for E_{corr} but not lower values for i_{corr}

$$i_{corr,est} = i_{corr,0} + c \cdot t + \frac{\Delta_{st}}{r} \quad (4)$$

Cover concrete remained sound during the first 3 years of marine exposure. After that, oxide patterns in coincidence with reinforcement bars began being noticed. This period coincides with the stabilization of the corrosion rate near 38 months of exposure (Fig. 9). From this moment, the increasing term in Eq. 4 was disregarded, and the value of $i_{corr,0}$ was replaced by the stabilized value of the corrosion rate, $i_{corr,1}$ = 4.7 μA/cm^2.

The values for the parameters used in the model (Eqs. 2–4) are not appropriate to concrete properties and/or exposure conditions different from those presented in this paper. However, the proper values may be obtained from previous data of corrosion and climate parameters in the same structure under study or other under equivalent circumstances.

At the exposure period of 57.8 months, a detailed examination of cracks (lines) and oxide patterns (shaded zones) was performed (Fig. 10). It should be remembered that the faces named 'A' were at the top during exposition, 'C' faces were at the bottom, and 'B' and 'D' faces were lateral. Corrosion-induced cracking of concrete involves two major stages. At the beginning of the active corrosion process, a layer of corrosion products is formed at the interlayer between concrete and steel. This causes disbondment at the interface. When the disbondment stage is advanced, cracks and/or spalls of cover concrete are formed. The visual inspection of concrete members allows asserting that the volume of corrosion products was larger enough to cause major failings in spite of the relatively short exposure term of 57.8 months (in comparison with the service life of a real structure).

The external signs of corrosion do not necessarily reflect the total extent of damage. If concrete contains a substantial volume of interconnected pores and voids, they may act as repositories for corrosion products and increase the time for cracking or avoid any cracking at all. The concrete used was of low quality, and a corresponding hiding of damage may be reasonably assumed.

5 Conclusions

Environmental actions on the corrosion rate of active steel in concrete made with BPC exposed in a marine environment were experimentally assessed. An exposure period of 4.8 years was analyzed, and a direct relationship between the corrosion rate and ambient temperature and RH was derived.

Variations of ambient humidity and temperature affected both the half-cell potential and the corrosion rate of reinforcement. Cyclic sine variation of the half-cell potential was found. This variation is mainly attributed to the varying moisture content of concrete due to environmental actions. On the other hand, corrosion rate progressed with time, but a season effect on the extent of the increase was also considered. Conceptually opposite seasonal effects on the half-cell potential and the corrosion rate of active steel embedded in concrete were found.

The parameter temperature multiplied by the RH is proposed as a quantifier for the environmental actions on the half-cell potential and the corrosion rate. This proposal fit consistently to the obtained results. Therefore, a direct link between the climatic actions and the deterioration rate was quantitatively established.

For each exposure period, both half-cell potential and corrosion rate showed variations in their values

due to concrete heterogeneity and orientation of the concrete surface. This affectation was higher for the corrosion rate than for the half-cell potential.

References

1. Frederiksen JM, Sørensen HE, Andersen A, Klinghoffer O (1997) HETEK, The effect of the w/c ratio on chloride transport into concrete—immersion, migration and resistivity tests. The Road Directorate, Copenaguen
2. ASTM C876 (2009) Standard test method for corrosion potentials of uncoated reinforcing steel in concrete. ASTM International, West Conshohocken, USA
3. Broomfield JP (1997) Corrosion of steel in concrete—understanding, investigation and repair. E & FN SPON, London
4. Stratfull RF (1973) Corrosion autopsy of a structurally unsound bridge deck. Highw Res Rec 433:1–11
5. Andrade C, González JA (1978) Quantitative measurements of corrosion rate of reinforcing steels embedded in concrete using polarization resistance measurements. Mater Corr 29:515–519. doi:10.1002/maco.19780290804
6. Bertolini L, Elsener B, Pedeferri P, Polder R (2003) Corrosion of steel in concrete. prevention, diagnosis, repair. Wiley-VCH, Weinheim
7. Alonso C, Castellote M, Andrade C (2002) Chloride threshold dependence of pitting potential of reinforcements. Electrochim Acta 47:3469–3481. doi:10.1016/s0013-4686(02)00283-9
8. Andrade C, Alonso C (1996) Corrosion rate monitoring in the laboratory and on-site. Constr Build Mater 10:315–328. doi:10.1016/0950-0618(95)00044-5
9. Clear KC (1989) Measuring rate of corrosion of steel in field concrete structures. Transport Res Rec 1211:28–37
10. López W, González JA (1993) Influence of the degree of pore saturation on the resistivity of concrete and the corrosion rate of steel reinforcement. Cem Concr Res 23:368–376. doi:10.1016/0008-8846(93)90102-F
11. Enevoldsen JN, Hansson CM, Hope BB (1994) The influence of internal relative humidity on the rate of corrosion of steel embedded in concrete and mortar. Cem Concr Res 24:1373–1382. doi:10.1016/0008-8846(94)90122-8
12. Andrade C, Alonso C, Sarría J (1998) Influencia de la humedad relativa y la temperatura en las velocidades de corrosión de estructuras de hormigón. Mater Constr 251:5–17. doi:10.3989/mc.1998.v48.i251.468